The geometry of Tipping Points

Colleen M. Farrelly*
Post Urban Ventures
Miami Florida, USA

Yaé Ulrich Gaba†
Dept. of Math. and Applied Math.
Sefako Makgatho Health Sciences University
Pretoria, South Africa

Franck Kalala Mutombo‡
Dept. of Math. and Comp. Sci.
University of Lubumbashi
Lubumbashi, DRC

February 20, 2025

Abstract

In this work, we explore alternative graph-based metrics to discrete Ricci curvature for stock and goods market tipping point identification. Specifically, we investigate the graph Euler characteristic, graph Laplacian energy, and the zeta function derivative of graph Laplacian non-zero eigenvalues. We find that all our proposed metrics correlate well with Forman-Ricci curvature and that the graph Euler characteristic has favorable computational cost.

keywords- Graph-based metrics, discrete Ricci curvature, tipping point identification, graph Euler characteristic, graph Laplacian energy, zeta function derivative, financial networks, stock market, goods market, Forman-Ricci curvature, network analysis.

1 Introduction

Change point detection is an important task in time series analytics [1]. Within the context of economics, market fragility can have wide-ranging impacts on employment, international market and sociopolitical stability, and goods pricing [2, 4, 9]. These disproportionately impact emerging and frontier economies, where market fragility and impacts from international market volatility can impact food security [4]. Previous work on market fragility indicators includes recent work on the use of graph metrics to understand market sector correlation and cross-correlation [9]. One promising graph metric is discrete Ricci curvature, which measures the extent that vertices connected to other vertices via edges are warped and weighed down by those connections in that region of the graph [9]; however, computing the two main forms of discrete Ricci curvature Forman-Ricci curvature and Ollivier-Ricci curvature are computationally intensive and may not scale well enough to large scale analyses [13]. In this work, we explore alternative graph metrics including graph Euler characteristic, graph Laplacian energy, and zeta function derivatives of graph Laplacian non-zero eigenvalues as potential alternatives to discrete Ricci curvature. We also expand the original work on stock market fragility to a spatiotemporal dataset involving volatile millet pricing.

2 Methods

2.1 Analytics tools

2.1.1 Forman-Ricci Curvature

The Forman-Ricci curvature provides a discrete analog of Ricci curvature, making it particularly useful in the study of graphs and networks. It plays a crucial role in understanding the geometric properties of data structures, as demonstrated

*cfarrelly786@gmail.com
†yaeulrich.gaba@gmail.com
‡mutombof@unilu.ac.cd

in Beuria?s work on collider observations [18] and Weber et al.'s exploration of network geometry [20]. By analyzing the curvature of edges in a graph, this concept helps detect structural anomalies and provides insights into data connectivity, robustness, and clustering in topological data analysis [17]. In differential geometry, Ricci curvature describes how much the volume of a geodesic ball deviates from that in flat Euclidean space. For graphs, **Forman-Ricci curvature** provides a discrete analog by quantifying how much an edge in a network "spreads out" the connections of its vertices. This curvature value helps highlight regions of stability or potential tipping points in a network or a graph.

Without loss of generality, a graph is considered here as a pair $G = (V, E)$, where V is a set of vertices or nodes, and E is a set of edges between the vertices, $E \subseteq \{(u, v)|u, v \in V\}$. A graph may be undirected, that is edges have no orientation or it may be directed, that is edges have direction. The order of a graph G, denoted as $|G|$, is the number of vertices of that graph. On the other hand, the number of edges of a graph is denoted by $\|G\|$. The order (or size) of a graph determines whether it is finite or infinite. For a simple finite network $G = (V, E)$, the adjacency matrix $\mathbf{A}(\mathbf{G})$ is an $n \times n$ matrix with entries such that

$$A_{ij} = \begin{cases} 1 & \text{if there is an edge between vertices } v_i \text{ and } v_j, \\ 0 & \text{otherwise.} \end{cases} \tag{2.1}$$

The degree matrix is a diagonal matrix that provides information about the degree of each node in a given network. Given a network $G = (V, E)$ with $n = |V|$, the degree matrix $\mathbf{D}(\mathbf{G})$ is defined as

$$D_{i,j} = \begin{cases} k_i & \text{if } i = j \\ 0 & \text{otherwise.} \end{cases} \tag{2.2}$$

In a graph $G = (V, E)$ with vertices V and edges E, Forman-Ricci curvature provides a way to analyze "tight" (positive curvature) versus "loose" (negative curvature) connections. High positive curvature suggests stable clusters, while negative curvature indicates points where perturbations can propagate, signaling areas of instability and potential tipping points.

For a smooth Riemannian manifold, the Ricci curvature tensor $\mathrm{Ric}(X, X)$ measures how a geodesic emanating from a point p diverges or converges, providing insights into the local shape of the manifold. Positive Ricci curvature generally implies that geodesics converge, indicating stability, while negative Ricci curvature suggests divergence.

In Forman's discrete version, we assign the curvature to each edge based on the local structure around the edge's endpoints. This discrete curvature $F(e)$ for an edge e connecting vertices v_1 and v_2 in a graph G can be calculated using weights associated with edges and vertices.

For an edge e, Forman-Ricci curvature is defined as:

$$F(e) = w(e) \left(\frac{w(v_1)}{w(e)} + \frac{w(v_2)}{w(e)} - \sum_{e_i \sim v_1} \frac{w(v_1)}{\sqrt{w(e)w(e_i)}} - \sum_{e_j \sim v_2} \frac{w(v_2)}{\sqrt{w(e)w(e_j)}} \right) \tag{2.3}$$

where:

- $w(e)$ is the weight of edge e.
- $w(v_1)$ and $w(v_2)$ are the weights of vertices v_1 and v_2 connected by e.
- The notation $e_i \sim v_1$ means that e_i is an edge incident to v_1, and similarly for $e_j \sim v_2$.
- **Positive curvature**: If $F(e) > 0$, this edge is in a stable part of the network, where connections tend to cluster, reinforcing local stability.
- **Negative curvature**: If $F(e) < 0$, this edge is in an unstable part of the network, where local perturbations are likely to propagate, potentially leading to tipping points.

These positive and negative regions of curvature help to identify clusters and bottlenecks in the network structure.

The illustration below demonstrates a simple graph with two vertices connected by an edge, showing how to compute Forman-Ricci curvature on a basic structure.

Consider the following weights:

- $w(e) = 1$ (edge weight between v_1 and v_2),
- $w(v_1) = 2$ and $w(v_2) = 3$,
- Incident edge weights: $w(e_1) = 1$, $w(e_2) = 1$, $w(e_3) = 2$, $w(e_4) = 2$.

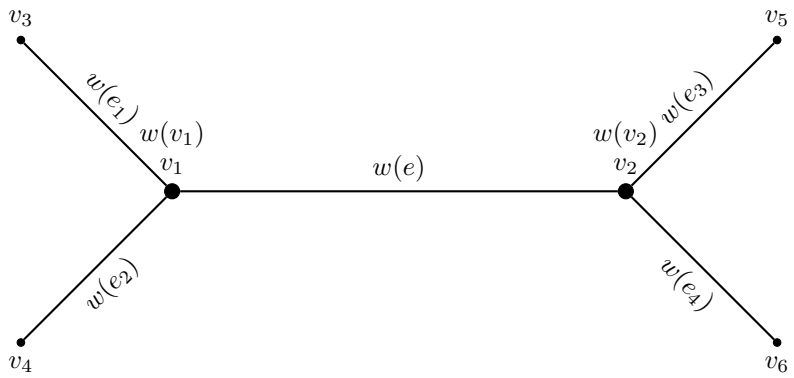

Figure 1: Forman-Ricci curvature calculation on a simple graph with vertices v_1 and v_2 connected by an edge e.

Plugging these values into the formula (2.3):

$$F(e) = 1\left(\frac{2}{1} + \frac{3}{1} - \frac{2}{\sqrt{1\cdot 1}} - \frac{2}{\sqrt{1\cdot 1}} - \frac{3}{\sqrt{1\cdot 2}} - \frac{3}{\sqrt{1\cdot 2}}\right)$$

Simplify each term:

$$F(e) = 1\left(2 + 3 - 2 - 2 - \frac{3}{\sqrt{2}} - \frac{3}{\sqrt{2}}\right) = 1\left(1 - \frac{6}{\sqrt{2}}\right)$$

The resulting curvature depends on the specific values, but will indicate a positive or negative curvature based on the configuration.

2.1.2 Graph Euler characteristic

The graph Euler characteristic is a fundamental invariant that captures the topological complexity of networks and is widely used in topological data analysis and shape recognition [19]. It serves as a key descriptor in understanding the combinatorial structure of datasets, as illustrated in the work of Luckhardt [21], which examines its relationship with volume comparison theorems. The Euler characteristic is particularly relevant when studying higher-dimensional graphs, where it helps characterize holes, connectivity patterns, and topological persistence.

This section explores the graph Euler characteristic as a topological invariant, offering insights into the global structure of a network. By connecting the Euler characteristic with curvature and homology, this section shows how topology and geometry intersect to detect tipping points.

The Euler characteristic $\chi(G)$ for a graph G is defined as:

$$\chi(G) = V - E \tag{2.4}$$

where V is the number of vertices and E is the number of edges.

In higher dimensions, using homology, we generalize as follows:

$$\chi(G) = \sum_{k=0}^{n} (-1)^k \beta_k \tag{2.5}$$

where β_k represents the k-th Betti number, counting k-dimensional homology classes (connected components, loops, and higher dimensional voids).

To extend the Euler characteristic χ to higher dimensions, we use the concepts of homology and Betti numbers, which count specific topological characteristics in each dimension.

2.2 Homology and Betti mumbers

Homology and Betti numbers provide deeper insights into the topology of data by quantifying the number of connected components, cycles, and higher-dimensional voids [22]. These tools have been essential in manifold learning and TDA, especially in applications to positive Ricci curvature and geometric structures, as seen in the work of Jiang and Yang [23]. By computing Betti numbers, researchers can effectively classify shapes and patterns in complex datasets, making these concepts crucial for studying high-dimensional data representations and persistent homology [17].

In topology, **homology** measures "holes" in different dimensions:

- **0-dimensional homology** (H_0) corresponds to connected components.
- **1-dimensional homology** (H_1) corresponds to loops or cycles.
- **2-dimensional homology** (H_2) corresponds to voids (e.g., the hollow inside a sphere).

For a given dimension k, the k-th **Betti number** β_k counts the number of independent k-dimensional cycles or holes. The Euler characteristic formula can then be extended as follows:

$$\chi = \sum_{k=0}^{n} (-1)^k \beta_k \tag{2.6}$$

where:

- β_0 counts connected components.
- β_1 counts loops or cycles.
- β_2 counts voids, etc.

In essence, the Euler characteristic sums up these Betti numbers, alternating signs to account for their dimensionality.

Definition 2.3. *A **simplicial complex** is a collection of simplices (vertices, edges, triangles, etc.) that represents the structure of a topological space in discrete terms. Each simplex contributes to the Euler characteristic based on its dimension:*

$$\chi = \sum_{k=0}^{n} (-1)^k f_k \tag{2.7}$$

where f_k is the number of k-dimensional simplices:

- f_0*: vertices*
- f_1*: edges*
- f_2*: triangles*
- f_3*: tetrahedra, and so on.*

Using the relationship between simplices and homology, we can show that each simplex relates to specific Betti numbers through boundary and coboundary relationships.

Below is an illustration that visualizes Betti numbers up to the 2-dimensional case:

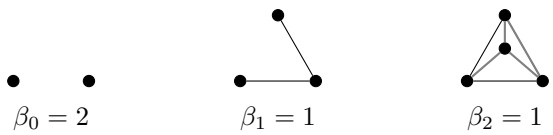

Figure 2: Illustrating Betti numbers: connected components (β_0), loops (β_1), and voids (β_2).

To demonstrate, let us calculate the Euler characteristic for a complex with these features:

- **2 vertices** for Betti 0: $\beta_0 = 2$
- **1 loop** for Betti 1: $\beta_1 = 1$
- **1 void** for Betti 2: $\beta_2 = 1$

Then, applying the formula:

$$\chi = \sum_{k=0}^{2} (-1)^k \beta_k = \beta_0 - \beta_1 + \beta_2 = 2 - 1 + 1 = 2. \tag{2.8}$$

This Euler characteristic tells us that, topologically, the space behaves like a connected complex with no other higher-dimensional holes.

This approach, with Betti numbers and the Euler characteristic, extends to complex systems where tipping points may be related to changes in homology. In higher dimensions, such changes might correspond to the merging or splitting of components (H_0), the formation of new cycles (H_1), or the creation / closing of voids (H_2 and beyond), which may signal structural shifts in the system.

The illustration visually aids understanding by mapping these homology features in terms of Betti numbers, enhancing comprehension of the Euler characteristic's role in topology and complex systems.

In discrete settings, analogues of the Gauss-Bonnet theorem relate the global Euler characteristic to sums of local curvature. If $K(v)$ denotes the curvature at a vertex v, then:

$$\sum_{v \in V} K(v) = \chi(G) \tag{2.9}$$

The distribution of Forman-Ricci curvature influences the global topology, impacts the Euler characteristic, and indicates changes in system structure.

2.4 Graph Euler characteristic and homology in tipping points

Sudden changes in the Euler characteristic can occur due to the creation or destruction of edges, indicating shifts in the network's connectivity. These changes often signal **tipping points**, where the system undergoes a qualitative transition, such as a change from stability to instability.

The Euler characteristic can be expressed in terms of Betti numbers:

$$\chi = \beta_0 - \beta_1 + \beta_2 - \dots$$

Changes in homology provide critical insights into network resilience:

- **Emergence of Loops (β_1)**: Suggests the formation of clusters or cycles, which can act as stabilizing structures but may also indicate vulnerabilities.
- **Collapse of Loops or Components (β_0)**: Signals fragmentation or disconnection, often associated with instability or the breakdown of network coherence.

Visualizing Euler Characteristic and Homology

To illustrate these concepts, consider the following example:

Example: A simple stock network

Below is a sequence of graphs showing how the Euler characteristic and homology change as the network evolves.

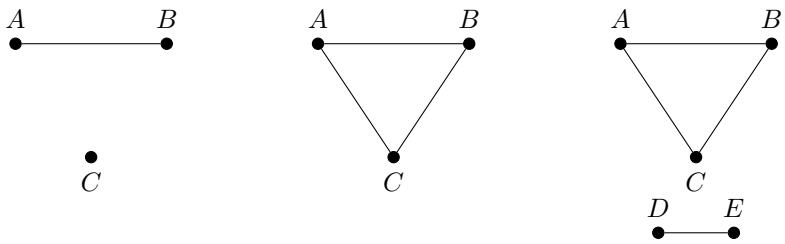

Figure 3: Evolution of a simple stock network.

- **Graph 1**: Two connected nodes with one isolated node ($\chi = 2$, $\beta_0 = 2, \beta_1 = 0$).

- **Graph 2**: All nodes are connected, forming a single loop ($\chi = 1$, $\beta_0 = 1, \beta_1 = 1$).
- **Graph 3**: A second loop appears, indicating the formation of a new cluster ($\chi = 0$, $\beta_0 = 1, \beta_1 = 2$).

Observing tipping points

In the above sequence:

- The transition from Graph 1 to Graph 2 represents a **tipping point**, where the network shifts from being fragmented ($\beta_0 = 2$) to cohesive ($\beta_0 = 1$) but introduces new cycles ($\beta_1 = 1$).
- The emergence of a second loop in Graph 3 suggests increased clustering, potentially stabilizing the system but also highlighting areas of interdependency.

Applications in stock market networks

In stock market networks, the Euler characteristic and homology offer valuable insights into market stability:

1. **Clusters and Cycles**: Identify groups of stocks with similar behaviors or mutual reinforcement.
2. **Network Fragmentation**: Detect when market coherence breaks down, signaling potential tipping points or sector decoupling.
3. **Monitoring Stability**: Changes in β_0 or β_1 can indicate shifts in market dynamics, such as the emergence of new correlations or the collapse of existing ones.

By combining topological invariants with other metrics like Forman-Ricci curvature and spectral analysis, we can gain a more comprehensive understanding of market resilience and the factors driving systemic risk.

2.5 Graph Laplacian Energy

The Laplacian matrix, sometimes called the admittance matrix or Kirchhoff matrix, is a matrix representation of a network. The Laplacian matrix provides useful information about the properties of a network. The Laplacian matrix of a network is the difference between the degree matrix $\mathbf{D}$ and the adjacency matrix $\mathbf{A}$ of a network. That is,

$$\mathbf{L} = \mathbf{D} - \mathbf{A}. \tag{2.10}$$

Given a simple network $G = (V, E)$, the entries of the Laplacian matrix $\mathbf{L}(\mathbf{G})$ are defined as

$$L_{ij} = \begin{cases} k_{v_i} & \text{if } i = j \\ -1 & \text{if } i \neq j \text{ and } v_i \text{ is adjacent to } v_j \\ 0 & \text{otherwise,} \end{cases} \tag{2.11}$$

where k_{v_i} denotes the degree of node i. Alternatively, we can define the Laplacian matrix of a graph in terms of the vertex-edge incidence matrix $\mathbf{B}$. That is,

$$\mathbf{L} = \mathbf{B}\mathbf{B}^T, \tag{2.12}$$

where $\mathbf{B}^T$ is the transpose of $\mathbf{B}$ For example Laplacian matrix of the network in Fig. 4.

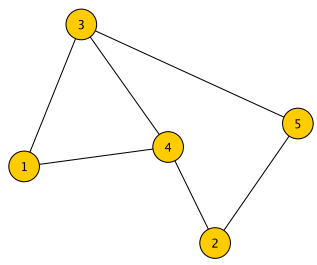

Figure 4: A Network G.

$$\mathbf{L} = \begin{pmatrix} 2 & 0 & -1 & -1 & 0 \\ 0 & 2 & 0 & -1 & -1 \\ -1 & 0 & 3 & -1 & -1 \\ -1 & -1 & -1 & 3 & 0 \\ 0 & -1 & -1 & 0 & 2 \end{pmatrix}. \tag{2.13}$$

The properties of the Laplacian matrix of a network are very useful in understanding the structure of a network. We therefore discuss some of these properties. The entries of the Laplacian matrix are real numbers and are symmetric concerning the main diagonal [12]. The Laplacian matrix is a square matrix that is not invertible. Its determinant is equal to zero [12]. The spectrum of the Laplacian provides useful information about the structure of a network. The spectrum of the Laplacian matrix is the set of all its eigenvalues and their multiplicities. Let $\lambda_1 < \lambda_2 < \ldots < \lambda_n$ be the distinct eigenvalues of $\mathbf{L}$ and let $m(\lambda_1), m(\lambda_2), \ldots, m(\lambda_n)$ be their multiplicities. Then, the spectrum of $\mathbf{L}$ is written as

$$Sp\mathbf{L} = \begin{pmatrix} \lambda_1 & \lambda_2 & \ldots & \lambda_n \\ m(\lambda_1) & m(\lambda_2) & \ldots & m(\lambda_n). \end{pmatrix} \tag{2.14}$$

Let us write the eigenvalues of $\mathbf{L}$ in decreasing order: $\lambda_n \geq \lambda_{n-1} \geq \cdots \geq \lambda_2 \geq \lambda_1 = 0$. Some of the results associated with the spectrum of the Laplacian matrix include:

- The eigenvalues of $\mathbf{L}$ are bounded as $0 \leq \lambda_j \leq 2k_{max}$ and $\lambda_n \geq k_{max}$.
- The eigenvalue λ_1 is always equal to zero [11].
- The multiplicity of 0 as an eigenvalue of $\mathbf{L}$ is equal to the number of connected components in the network.
- Every row sum and column sum of $\mathbf{L}$ is zero. Thus, the vector $\mathbf{v_1}$ of all ones is an eigenvector associated with $\lambda_1 = 0$, since $\mathbf{Lv_1} = \mathbf{0}$ [12].
- A network is connected if its second smallest eigenvalue is nonzero. That is, $\lambda_2 > 0$ if and only if G is connected. The eigenvalue λ_2 is thus called the algebraic connectivity of a network, $a(G)$. The eigenvector corresponding to the eigenvalue λ_2 is called the Fiedler vector [11],

We define here the Laplacian matrix of a weighted network. Let $G = (V, E, W)$ be a simple undirected weighted network with the vertex set $V(G) = \{v_1, v_2, \cdots, v_n\}$, edge set E, where each edge $e = (v_i, v_j)$ is attached with a weight w_{ij}. If there is no edge between v_i and v_j, $w_{i,j} = 0$. In addition, $w_{i,i} = 0$ and $w_{i,j} = w_{j,i}$. We define

$$\mathbf{W} = \begin{pmatrix} 0 & w_{1,2} & \ldots & w_{1,n} \\ w_{2,1} & 0 & \ldots & w_{2,n} \\ \vdots & \vdots & \vdots & \vdots \\ w_{n,1} & w_{n,2} & \ldots & 0 \end{pmatrix} \text{ and } \mathbf{X} = \begin{pmatrix} x_1 & 0 & \ldots & 0 \\ 0 & x_2 & \ldots & 0 \\ \vdots & \vdots & \vdots & \vdots \\ 0 & 0 & \ldots & x_n \end{pmatrix},$$

where x_i is the sum-weight of vertex v_i given by $x_i = \sum_{j=1}^{n} w_{i,j} = \sum_{u \in N(v_i)} w_{v_i,u}$, where $N(v_i)$ is the neighborhood of v_i.

The Weighted Laplacian matrix of a weighted network/graph G is the matrix

$$\mathbf{L} = \mathbf{X}(\mathbf{G}) - \mathbf{W}(\mathbf{G}), \tag{2.15}$$

and which can be seen as a generalization of (2.10).

Definition 2.6 (Laplacian Energy of a network)**.** *Let $G = (V, E, W)$ be a weighted network on n vertices and $\lambda_1, \lambda_2, \ldots, \lambda_n$ be the eigenvalues of its Laplacian matrix. The Laplacian energy of G is defined as*

$$E_L(G) = \sum_{i=1}^{n} \lambda_i^2.$$

As networks become larger, computing eigenvalues of the Laplacian matrix becomes very hard. We, therefore, use the entries of the Laplacian matrix rather than its eigenvalues to compute the Laplacian energy of a network. 2.7

Theorem 2.7. *For any network $G = (V, E, W)$ on n vertices whose vertex sum-weights are*

$x_1, x_2, \ldots, x_n$ *respectively, we have*

$$E_L(G) = \sum_{i=1}^{n} x_i^2 + 2\sum_{i<j} w_{i,j}^2. \tag{2.16}$$

The proof of this theorem can be found in [14].

2.8 Zeta function derivative

In this section, we introduce the zeta function associated with the Laplacian eigenvalues of a graph. We will be interested particularly in the derivative of the zeta function at the origin. To begin with, let us consider the function $f(t) = e^{-\lambda_i t}$, whose Mellin transform is given by:

$$F(p) = \int_0^\infty t^{p-1} f(t) dt, \tag{2.17}$$

and after a little algebraic transformation, we have:

$$\lambda_i^{-p} = \frac{1}{\Gamma(p)} \int_0^\infty t^{p-1} e^{-\lambda_i t} dt, \tag{2.18}$$

where λ_i is the i-th eigenvalue of the Laplacian matrix $\mathbf{L}_G$, and $\Gamma(p)$ represents the gamma function defined as:

$$\Gamma(p) = \int_0^\infty t^{p-1} e^{-t} dt. \tag{2.19}$$

Upon summing in Equation 2.18 for all non-zero eigenvalues of the Laplacian, the zeta function is given by:

$$\zeta(p) = \sum_{\lambda_i \neq 0} \lambda_i^{-p} = \frac{1}{\Gamma(p)} \int_0^\infty t^{p-1} \sum_{\lambda_i \neq 0} e^{-\lambda_i t} dt \tag{2.20}$$

The derivative of the zeta function associated with the Laplacian matrix is given by:

$$\zeta'(p) = \sum_{\lambda_i \neq 0} \{-\ln \lambda_i\} e^{-p \ln \lambda_i}. \tag{2.21}$$

At the origin, i.e., $p = 0$, we have

$$\zeta'(0) = -\sum_{\lambda_i \neq 0} \ln \lambda_i. \tag{2.22}$$

The derivative or slope of the zeta function at the origin is graph invariant of the heat kernel that can be used for graph characterization [15, 16] It is simpler than the zeta function because it is parameter-independent.

2.9 Data

We assessed our graph metrics' performance on two different datasets. To compare metrics in a purely temporal setting, we retrieved the NASDAQ stock dataset from Kaggle, including daily closing prices from Apple, Alphabet, Nvidia, Microsoft, American Airlines, LATAM Airlines, United States Steel, and Western Copper and Gold from May 19, 2006, to April 1, 2020. This included crashes in 2008 and 2020, as well as covered industries in tech, travel, and minerals. To compare metric performance on spatiotemporal data, we examined quarterly millet prices across Burkina Faso provinces from quarter 2 of 2015 to quarter 2 of 2015, which was originally collected by the World Food Programme Price Database. We filtered the dataset to include only millet prices and aggregated by quarter and province. We first created a time window for each dataset (5 days with a 4 day overlap for our stock data and 4 quarters with a 3 quarter overlap for our millet data). Then, we created an undirected graph for that time window by applying a value threshold (through a correlation threshold > 0.5 for our stock data and through a local Moran statistic > 0.9 for our Millet data). For the millet dataset, we chose spatial weights connecting provinces that share a border and used correlation as the metric. Finally, we calculated each of our chosen graph metrics for each time window graph to perform a correlation analysis of our metrics compared to Forman-Ricci curvature.

3 Results

The absolute value of our correlation coefficients across metrics were above 0.97 for all metric pairs in both our stock analysis and our food pricing analysis, which suggests that any of our proposed metrics can replace discrete Ricci curvature without impacting fragility analysis results. Further, because the graph Euler characteristic relies only on subtracting the number of edges from the number of vertices, which are stored in the graph structure, it is ideal for scaling fragility analysis to very large datasets. In addition, the graph Euler characteristic relates both curvature and homological properties through the Gauss-Bonnet Theorem, allowing insight into the local geometry and global topology of the system [5](Knill, 2012).

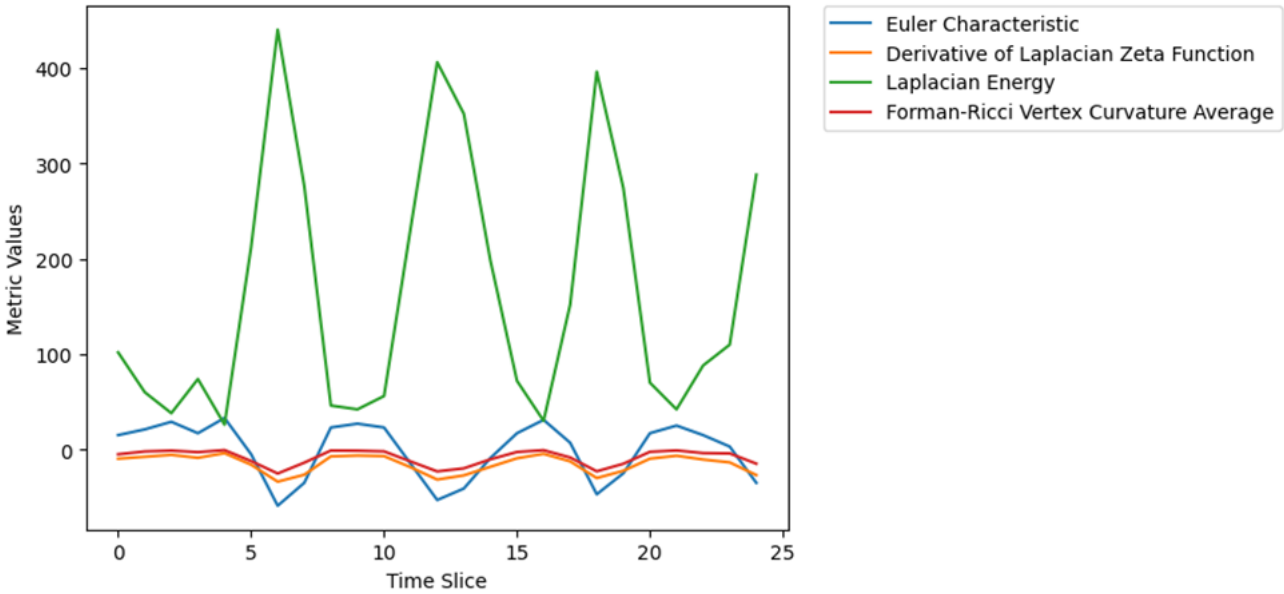

Figure 5: This image plots the windowed time series graph metric values (Euler characteristic, derivative of the Laplacian zeta function, Laplacian energy, and Forman-Ricci curvature) for the Burkina Faso millet dataset.

Figure 5 plots the Euler characteristic, derivative of the Laplacian zeta function, Laplacian energy, and Forman-Ricci curvature at each time window of the Burkina Faso millet dataset. Specific metrics tend to increase or decrease when other metrics increase or decrease, showing this strong correlation among our chosen graph metrics. The Euler characteristic tends to show a wider range of values compared to Forman-Ricci curvature, suggesting it also provides a good visualization tool of changing trends.

4 Discussion

We found that the graph Euler characteristic was a robust and computationally efficient alternative to discrete Ricci curvature and other computationally-intensive methods considered. It is likely to scale well to large-scale stock market prediction tasks involving thousands or millions of stocks over time. In addition, it performs well on spatiotemporal data, as well. We considered very few of the myriad graph theoretic tools and their extensions to higher-order networks such as hypergraphs, combinatorial complexes, or simplicial complexes. Our future work will explore more spectral and geometric tools that might explain the mechanisms of tipping points. Hodge Laplacians, which extend graph Laplacians to simplicial complexes via boundary operators, connect to Dirac operators, which measure system synchronicity [3]. In addition, topological and Clifford algebra neural networks may be useful in forecasting future trends in temporal and spatiotemporal data, such as stock market data [6]. In addition, graph and simplicial complex filtration has yielded successful tools like persistent homology and persistent Euler transforms [7]. Future works exploring persistent Euler characteristics, persistent spectral metrics, and other types of persistent graph and simplicial complex metrics are likely to add to our understanding of market fragility and tipping points.

References

[1] Aminikhanghahi, S., & Cook, D. J. (2017). A survey of methods for time series change point detection. Knowledge and information systems, 51(2), 339-367.

[2] Berger, D., & Pukthuanthong, K. (2012). Market fragility and international market crashes. Journal of Financial Economics, 105(3), 565-580.

[3] Chen, Y., Gel, Y. R., & Poor, H. V. (2022, June). BScNets: Block simplicial complex neural networks. In Proceedings of the aaai conference on artificial intelligence (Vol. 36, No. 6, pp. 6333-6341).

[4] Clapp, J., & Moseley, W. G. (2020). This food crisis is different: COVID-19 and the fragility of the neoliberal food security order. The Journal of Peasant Studies, 47(7), 1393-1417.

[5] Knill, O. (2012). A discrete Gauss-Bonnet type theorem. Elemente der Mathematik, 67(1), 1-17.

[6] Papillon, M., Bernárdez, G., Battiloro, C., & Miolane, N. (2024). TopoTune: A Framework for Generalized Combinatorial Complex Neural Networks. arXiv preprint arXiv:2410.06530.

[7] Roell, E., & Rieck, B. (2023). Differentiable Euler characteristic transforms for shape classification. arXiv preprint arXiv:2310.07630.

[8] Ruhe, D., Brandstetter, J., & Forré, P. (2024). Clifford group equivariant neural networks. Advances in Neural Information Processing Systems, 36.

[9] Sandhu, R. S., Georgiou, T. T., & Tannenbaum, A. R. (2016). Ricci curvature: An economic indicator for market fragility and systemic risk. Science advances, 2(5), e1501495.

[10] R. Forman; *Bochner's Method for Cell Complexes and Combinatorial Ricci Curvature*, Discrete and Computational Geometry, 2003, 29(3): 323-374.

[11] Estrada, E. The structure of complex networks: theory and applications. (OUP Oxford,2011)

[12] Das, K. The Laplacian spectrum of a graph. *Computers and Mathematics With Applications.* **48**, 715-724 (2004).

[13] J. Jost and S. Liu; *Ollivier's Ricci Curvature, Local Clustering and Curvature-Dimension Inequalities on Graphs*, Discrete Mathematics, 2014, 338(1): 23-36.

[14] Gower, J. A modified Leverrier-Faddeev algorithm for matrices with multiple eigenvalues. *Linear Algebra And Its Applications.* **31** pp. 61-70 (1980)

[15] Kalala Mutombo, F. & Nanyanzi, A. Generalised heat kernel invariants of a graph and application to object clusteringImage 1. *Computers and Mathematics With Applications*, **167** pp. 264-285 (2024).

[16] Kalala Mutombo, F., Nanyanzi, A. & Utete, S. Heat Kernel of Networks with Long-Range Interactions. *Complexity.* **2024**, 6745905,

[17] Farrelly, C. M., & Gaba, Y. U. (2023). *The Shape of Data: Geometry-Based Machine Learning and Topological Data Analysis.* No Starch Press. https://www.amazon.ca/Shape-Data-Geometry-Based-Learning-Topological/dp/1718503083

[18] Beuria, J. Intrinsic geometry of collider observations and Forman Ricci curvature. *Physical Review D.* **110**, 035023 (2024), https://doi.org/10.1103/PhysRevD.110.035023

[19] Hacquard, S. & Lebovici, J. Euler Characteristic Tools for Topological Data Analysis. (2024), https://hal.science/hal-04143938/document

[20] Weber, M., Saucan, E. & Jost, J. Can one see the shape of a network?. (2016), https://arxiv.org/abs/1608.07838

[21] Luckhardt, D. A volume comparison theorem for characteristic numbers. (2020), https://arxiv.org/abs/2005.06884

[22] Wei, G. Ricci Curvature and Betti Numbers. (1994), https://arxiv.org/abs/dg-ga/9411003

[23] Jiang, H. & Yang, Y. Manifolds of positive Ricci curvature, quadratically asymptotically nonnegative curvature, and infinite Betti numbers. (2019), https://arxiv.org/abs/1905.01616